Scientific Research Publishing

Comprehensive Analysis of CuIn$_{1-x}$Ga$_x$Se$_2$ Based Solar Cells with Zn$_{1-y}$Mg$_y$O Buffer Layer

**Soumaïla Ouédraogo[1,2]*, Marcel Bawindsom Kébré[1],
Ariel Teyou Ngoupo[2], Daouda Oubda[1], François Zougmoré[1]**

[1]Laboratoire de Matériaux et Environnement (LA.M.E)-UFR/SEA, Université Joseph Ki-ZERBO, Ouagadougou, Burkina Faso
[2]Département de Physique, Faculté des Sciences, Université de Yaoundé I, Yaoundé, Cameroun
Email: *ouedraogosoumaila1@gmail.com

Abstract

The development of cadmium-free CIGS solar cells with high conversion efficiency is crucial due to the toxicity of cadmium. Zinc-based buffer layers seem to be the most promising. In this paper, a numerical analysis using SCAPS-1D software was used to explore the Zn(Mg,O) layer as an alternative to the toxic CdS layer. The effect of several properties such as thickness, doping, Mg concentration of the Zn(Mg,O) layer on the current-voltage parameters was explored and their optimal values were proposed. The simulation results reveal that the optimal value of the ZMO layer thickness is approximately 40 nm, the doping at 10^{17} cm^{-3} and an Mg composition between 0.15 and 0.2. In addition, the effect of Gallium (Ga) content in the absorber as well as the Zn(Mg,O)/CIGS interface properties on the solar cell's performance was examined. The results show that contrary to the CdS buffer layer, the best electrical characteristics of the ZMO/CIGS heterojunction are obtained using a Ga-content equal to 0.4 and high interface defect density or unfavorable band alignment may be the causes of poor performances of Zn(Mg,O)/CIGS solar cells in the case of low and high Mg-contents.

Keywords

Device Modeling, Zn(Mg,O), Cu(In,Ga)Se$_2$, Interface Sates, Conduction Band Offset

1. Introduction

Recently, Cu(In,Ga)Se$_2$ thin film solar cells with conversion efficiency of 23.35% have been reported in literature for laboratory cells [1], and commercial modules are now fabricated by large quantities. In these solar cells, CdS deposited by

chemical bath deposition (CBD) is widely used as buffer layer to form a p-n heterojonction between n-CdS and p-CIGS. One of the key factors for obtaining a record efficiency of polycrystalline CIGS based solar cells is related to the presence of high quality p-n heterojonction between CdS buffer layer and CIGS absorber. However, the use of CdS is undesirable in large-scale production of CIGS solar cells because of its toxicity [2]. Moreover, the decrease in the short circuit voltage due to the optical absorption of the short wavelengths by the CdS layer is a concern for the scientific community of CIGS solar cells [3]. In any case, it is in the interest of the scientific community to find an alternative to this toxic buffer layer. However, the replacement of the CdS layer by Cd-free materials is a hard puzzle because it is not merely a question to replace the CdS with fantasy, but to find a compromise between the cost of the resulting cells and its effectiveness. Employing a wide band-gap buffer layer is a possible route to solve this problem. Among the many alternative materials offered by different laboratories, Zn-based compounds appear to meet the requirements in terms of cost and efficiency. Thus, most attention is focused on zinc oxide (ZnO) due to its potential applications as transparent conducting films for different optoelectronic devices such as liquid crystal displays and solar cells. ZnO thin films have already been used as an alternative to the highly toxic CdS layers in $CuInGaSe_2$ based solar cells. However, there are some limitations in the application of ZnO in thin film solar devices since its band gap is not wide enough. In addition, the negative conduction band offset of −0.2 eV at the ZnO/CIGS interface is assumed to affect cell performance [4]. As a result, a tunable band-gap material such as $Zn_{1-x}Mg_xO$ (ZMO) has recently received a lot of attention. The advantage of this buffer layer is that its conduction band can be adjusted to optimize the band alignment at the buffer layer/absorber interface. Previous works have shown that ZMO could be an alternative as Cd-free buffer layer in CIGS solar cells [5]. An improvement of the short-current density (J_{sc}) was observed in the CIGS solar cells with ZMO buffer layer. In comparison to the conventional CdS buffer layer, the best solar cells with the Zn(Mg,O) buffer layer have lower V_{oc} and FF [6]. The combination of the ZMO layer with another Zn-based window layer has been proposed to reduce the absorption of short wavelengths and recombination at the buffer layer/absorber interface.

Hariscos *et al.* obtained an efficiency of 18% using the ZnS/ZMO combination as a buffer layer [7]. Saadat *et al.* studied the Zn(O,S)/Zn(Mg,O) combination and proposed an optimal oxygen and magnesium compositions for high efficiency [8]. More recently, a record efficiency of Cd-free CIGS solar cells has been achieved using the Zn(O,S,OH)/ZMO combination [1]. The reduction of V_{oc} deficit, increase in J_{sc} and FF was highlighted as the key to the success of this combination [1]. Even though this combination allows to achieve high conversion efficiency CIGS solar cells, the technological process is complicated since usually the juxtaposed buffer layers are not deposited by the same process [1] [7].

In this paper, device modeling and simulation using SCAPS-1D software [9] were conducted to investigate the effect ZMO mono-buffer layer on the performance of the CIGS solar cell. Optimal properties of the ZMO layer such as thickness, donor density, magnesium concentration were proposed. In addition, ZMO/CIGS interface properties have been studied to elucidate how they affect device performance. The simulation results suggest that, high interface defect density and unfavorable band alignment may be the causes of poor performances of Zn(Mg,O)/CIGS solar cells in the case of low and high Mg-contents. A comparison of the simulation results with published data for CIGS cells with Zn(Mg,O) buffer layer shows an excellent agreement.

2. Materials and Methods

In this study, the solar cell is in the configuration ZnO:B/i-ZnO/ZMO/SDL/ CIGS/Mo/substrate (Figure 1(a)). The conventional CdS layer was replaced by ZMO layer in the form $Zn_{1-y}Mg_yO$ where y in the concentration of Mg atoms denoted Mg-content. The SDL layer, generally referred to as the Surface Defect Layer (SDL), is formed on the absorber surface due to the diffusion of atoms at the CdS/absorber interface. Polycrystalline solar cells like CIGS are complicated structure due to the number of layers and the fact that the effect of some particular phenomena or material parameters often results from institution. Today, computer-aided design has become an important strategy to explore efficiently complex structures. Using a powerful device simulator, one can understand and predict the effect of the variation of the material parameters and propose optimal values to optimize the solar cell efficiencies and give the manufactures additional ideas to improve performance. Several one -dimensional software, among which SCAPS-1D [9], AMPS-1D [10], ASA [11], PC-1D [12], AFORS-HET [13], have been developed to simulate thin-film solar cells such as CdTe, CIGS and a-Si:H. In this work, computational analysis was performed using SCAPS-1D program developed at the University of Gent [9]. SCAPS-1D calculates the internal electrical parameters of the solar cells using Poison's equation, electron
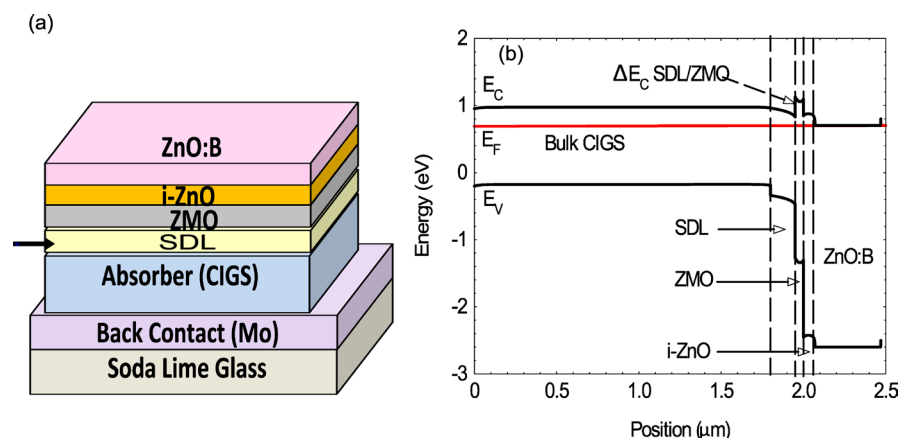

Figure 1. (a) Structure of the solar cell used in the simulation; (b) Band diagram in thermodynamic equilibrium.

and hole continuity equation by the coupled method of Newton-Raphson. Shockley-Read-Hall (SRH) model is used to calculate the recombination current for bulk defects and an extension of the SRH model for interface defect.

This work is a continuation of our previous paper, in which baseline parameters set for numerical simulation $Cu(In,Ga)Se_2$ in agreement with the experimental results was proposed [14]. In this work, only the buffer layer properties have been changed. Since CdS buffer layer was replaced by the ZMO layer, some adjustment of the buffer layer properties was made since there are likely to change when CdS is exchanged by ZMO layer [15]. The mobility and charge carrier concentrations as a function of Mg concentration in the ZMO layer are taken from experimental measurements [16]. Ga-grading in CIGS absorber is kept uniform and the absorption coefficient is set constant at 10^5 cm^{-1}. One type of single compensating mid-gap defects are introduced in each layer. The AM1.5 spectrum is used as the default illumination. The parameters of the different layers used in the simulation are summarized in Table 1. These parameters are largely obtained from the theoretical and experimental results of the literature [8] [15]-[20]. The equivalent band-diagram under equilibrium condition is given Figure 1(b).

Table 1. Input parameters values for simulating of CIGS solar cells with SCAPS-1D.

	Layer Properties				
	CIGS	SDL	ZMO	i-ZnO	ZnO:B
Layer thickness (nm)	2000	200	Variable	200	400
Layer band-gap: Eg (eV)	1.15	1.2	Variable	3.3	3.3
Electrons affinity: χ (eV)	4.5	4.5	Variable	4.55	4.55
Dielectric relative permittivity: $\varepsilon/\varepsilon_0$	13.6	13.6	10	9	9
Conduction band effective density of states: Nc (cm^{-3})	2.2×10^{18}	2.2×10^{18}	1.3×10^{18}	3.1×10^{18}	3×10^{18}
Valence band effective density of state: Nv (cm^{-3})	1.5×10^{19}	1.5×10^{19}	9.1×10^{18}	1.8×10^{19}	1.8×10^{19}
Electron thermal velocity: ν_e (cm/s)	3.9×10^7	3.9×10^7	3.1×10^7	2.4×10^7	2.4×10^7
Hole thermal velocity: ν_h (cm/s)	1.4×107	1.4×10^7	1.6×10^7	1.3×10^7	1.3×10^7
Electron mobility: μ_e (cm^2/Vs)	100	variable	72	100	100
Hole mobility: μ_h (cm^2/Vs)	12.5	1.25	20	31	31
Doping concentration (cm^{-3})	2×10^{16}	variable	5×10^{17}	10^{17}	1020
	Bulk defect properties				
Defect density and type: N (cm^{-3})	10^{14} (D)	Variable (D)	5×10^{16} (A)	10^{16} (A)	10^{16} (A)
Capture cross section electrons: σ_e (cm^2)	10^{-15}	10^{-13}	10^{-15}	10^{-15}	10^{-15}
Capture cross section electrons: σ_h (cm^2)	10^{-11}	10^{-15}	5×10^{-13}	5×10^{-13}	5×10^{-13}
	Interface properties				
Interface state	CIGS/SDL			SDL/ZMO	
Interface conduction band offset: ΔEc (eV)	0.3			variable	
Defect density and type: N (cm^{-2})	10^{11} (Neutral)			3×10^{13} (Neutral)	

3. Results and Discussion

3.1. Effect of ZMO Layer Thickness

The ZMO layer thickness is a critical parameter in the improvement of CIGS solar cell performances. It should allow the incident light to reach the absorber efficiently and contribute to reducing the series resistances at the ZMO/CIGS interface. Figure 2 shows the influence of the electrical parameters as a function of ZMO layer thickness. The open circuit voltage (V_{oc}) decreases almost linearly with the increase in the buffer layer thickness. The other parameters (J_{sc}, FF and Efficiency) remain almost stable for thin a buffer layer (<50 nm) and drop abruptly for thicknesses over 50 nm. The increase in the buffer layer thickness accentuates the absorption of photons in this layer and therefore a decrease of the spectral response at short wavelengths. The response of the solar cell is significantly better when the thickness of the buffer layer is lower. In this study, a thickness of 40 nm of the ZMO buffer layer is optimal for high efficiency.

3.2. Effect of ZMO Layer Donor Density

Figure 3 shows the effect of ZMO layer donor density on the performance of the solar cell. The configuration with or without the SDL layer is used in this simulation with acceptor defects at the CIGS/SDL interface. The pinning of the Fermi level results in the introduction of donor defects at the SDL/CdS interface, placed at 0.2 eV below the conduction band [20]. It can be seen that the behavior of the electrical parameters is strongly dependent on the interface configuration. V_{oc}, FF and efficiency remain high, stable independently of ZMO doping when the Fermi level is pinned. In this situation, high efficiency is achieved with the SDL layer. However, when the doping exceeds 10^{17} cm^{-3}, J_{sc} undergoes a strong decrease and slightly for conversion efficiency. This situation is certainly due to the increase in the reverse saturation current when the doping rate increases, the situation highlighted in [21]. Therefore, the value of 10^{17} cm^{-3} can be considered the optimal value of the ZMO layer doping.

3.3. Effect of Mg Concentration in the ZMO Layer

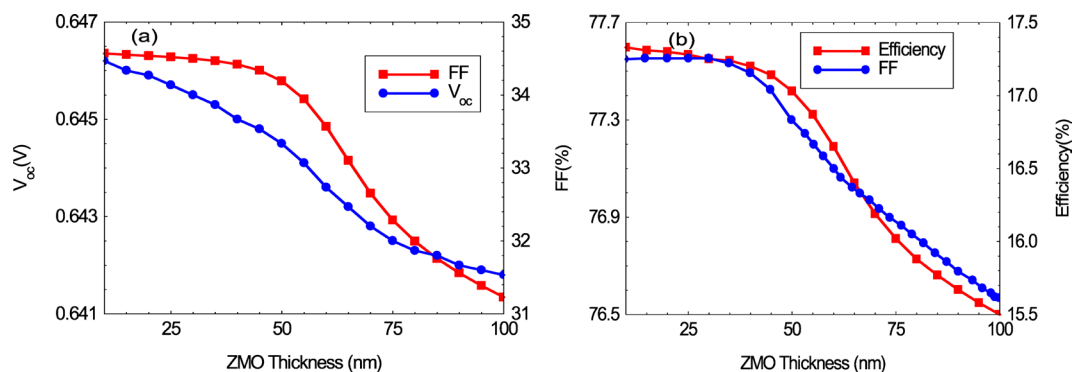In this part, all parameters of Table 1 are kept constant except the band-gap and

Figure 2. Effect of ZMO layer thickness on the electrical parameters V_{oc}, J_{sc}, FF and conversion efficiency.

the electronic affinity of the ZMO layer which have been introduced as variables. The relation between the performance of the solar as function Mg-concentration in the ZMO buffer layer is shown in **Figure 4**. The same trend is observed when
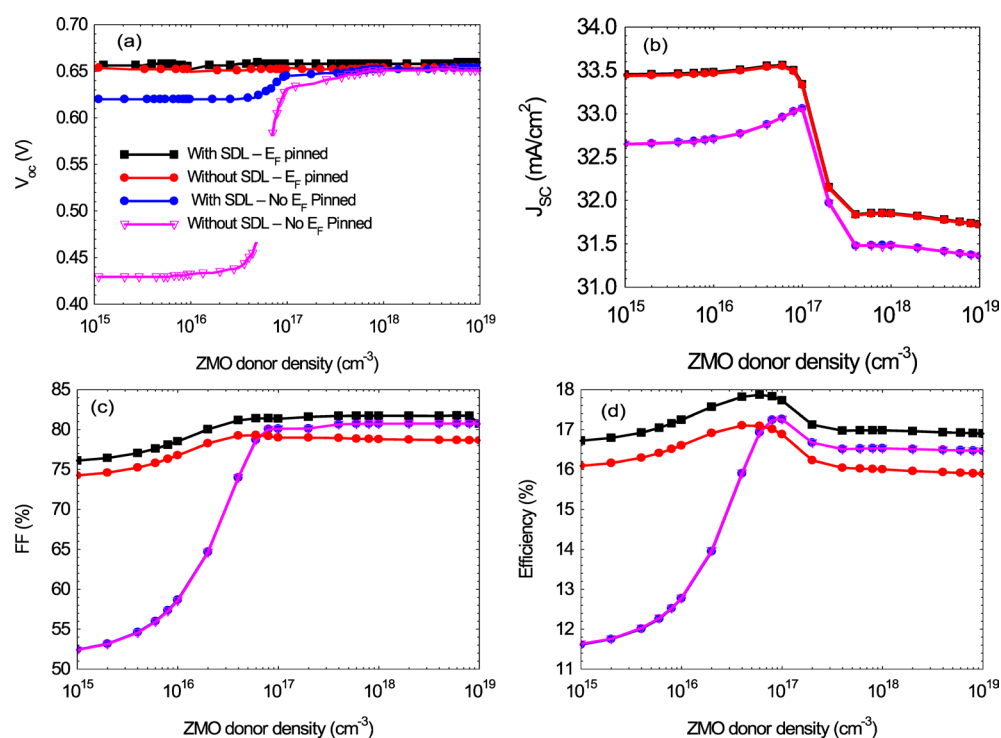

Figure 3. Effect of the ZMO layer doping on the electrical parameters depending on CdS/CIGS interface configuration.
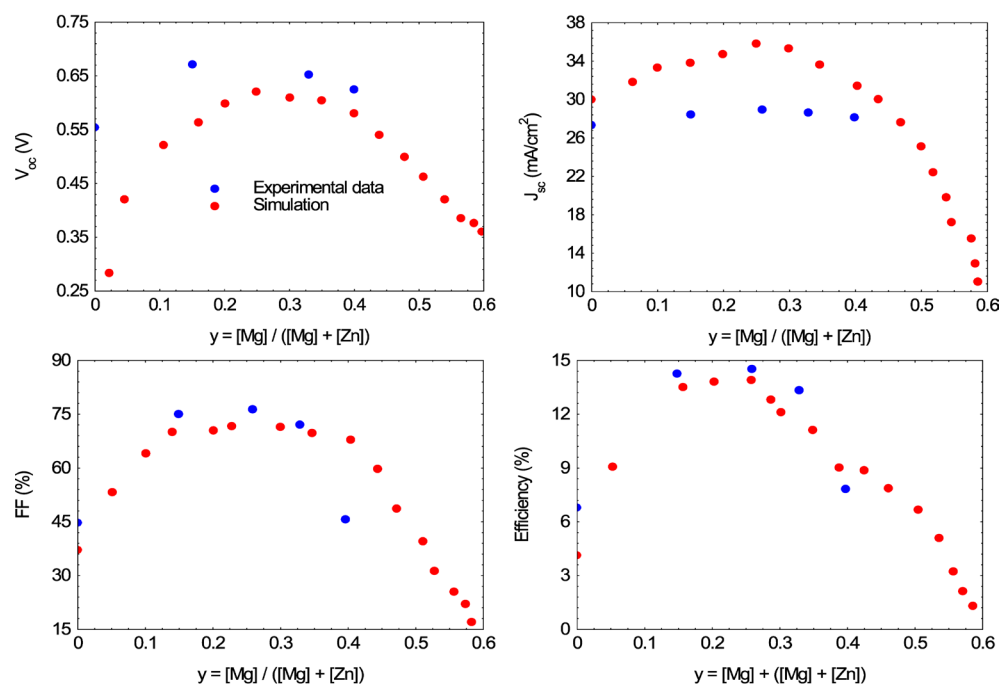

Figure 4. Trend of the electrical parameters as a function of Mg content in the ZMO layer. Experimental data are taken from Hariskos *et al.* [7].

the electrical parameters are plotted as a function of the ZMO layer band-gap. All the electrical parameters of the solar cells increase with the Mg-content in the buffer layer and reach their optimal value for $0.15 < y < 0.25$. However, when the Mg-content exceeds this optimal value, all parameters decrease. Cells with low Mg-content show poor electrical characteristics, mainly the open circuit voltage (V_{oc}) and fill factor (FF), which leads a low conversion efficiency. J_{sc} showed minor change for Mg-content between 0 - 0.15, but decreased drastically for $y > 0.25$. Computer analysis of CIGS solar cells with CdS buffer shows that the conduction band offset at the absorber/buffer layer interface is the main cause that reduces FF and J_{sc} due to a barrier against photo-generated electrons in the absorber [22]. The poor performance of the solar cell when $y < 0.15$ and $y > 0.25$ can be attributed to the high recombination rate at the absorber interface due to the mismatch of the conduction band offset [23] [24]. In **Figure 4**, the simulated electrical parameters are compared to the experimental data from Hariskos *et al.* for $0 < y < 0.4$ [7]. We founded very closed values for V_{oc}, FF and conversion efficiency except J_{sc} where slight deviations are observed.

By simultaneously set variable the Mg and Ga compositions in the ZMO and CIGS layers, we obtain the electrical parameters represented in contour plot in **Figure 5**. One can be seen that, the open circuit voltage (V_{oc}) is low for all Ga-content when Mg-content is lower than 0.1. Similarly, when Ga-content is lower than 0.15, the cell shows poor performance whatever the value of the Mg-content. This result is due to the mismatch of the conduction band offset between the buffer layer and the absorber, leading to degradation of ZMO/SDL interface quality and consequently the V_{oc}. The best V_{oc} of the ZMO/SDL/CIGS hetero-junction is obtained for Ga-content (x) higher than 0.15 and Mg-content (y) between 0.15 and 0.4. The short-circuit current density (J_{sc}) is optimal when
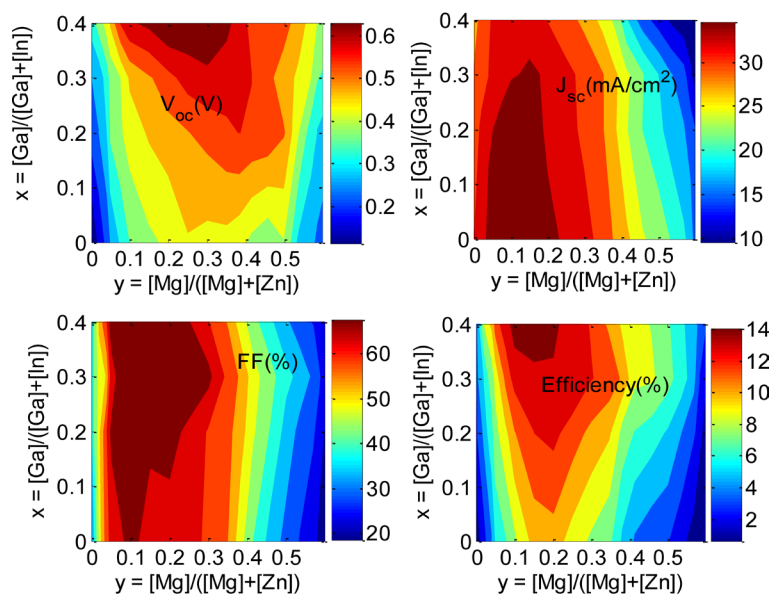

Figure 5. Electrical performance of CIGS base solar cells as a function of Ga-content (x) of the absorber and Mg-content (y) of the ZMO layer.

y is less than 0.4 regardless of the Ga-content (*x*) in the absorber. On the other hand, when y exceeds 0.3, J_{sc} decreases for all values of *x*. For 0.1 < *y* < 0.3, the fill factor (FF) is almost independent of the Ga-content and the best values of the fill factor are obtained. Beyond this range, we observe a decrease of the FF whatever the value of Ga-content. The best efficiencies are obtained for Ga-content range from 0.2 to 0.4 and Mg-content from 0.1 to 0.3 due to the mismatch of the conduction band offset.

3.4. Effect of Interface Configurations

Figure 6(a) shows the interface configurations in our numerical simulation. The interface properties considered are the defect densities at the Cu(In,Ga)Se$_2$/SDL (Interface I) and SDL/ZMO (Interface II) interfaces which link with the conduction band offset (CBO) at the SDL/ZMO interface (ΔEc(SDL/ZMO)). In this study, we didn't consider the conduction band offset at the ZMO/i-ZnO (ΔEc(ZMO/i-ZnO).

In **Figure 6(b)**, we plotted the variation of CBO at the SDL/ZMO interface as a function of the Mg-content. This conduction band offset at the SDL/ZMO interface was calculated by varying the ZMO layer electron affinity. A positive value of conduction band offset (Spike) indicates that the conduction band of the ZMO is above that of CIGS. The Spike acts as barrier against photo-generated electrons in Cu(In,Ga)Se$_2$ [19]. A negative value indicates that the conduction band (Cliff) of the ZMO layer is below that of CIGS. The cliff acts as a barrier against injected electrons form the n-type region and increase recombination via defects at the SDL/ZMO interface [23].

In a first step, the quality of the Cu(In,Ga)Se$_2$/SDL (Interface I) and SDL/ZMO (Interface II) interfaces was examined by varying the defect density of these two interfaces from 10^{12} to 10^{17} cm^{-2}. The band offsets at these interfaces were set to zero to avoid misanalysis due to the contribution of the band offsets.

We plotted in **Figure 7** the simulated electrical parameters as a function of the interface defect density. One can be seen that the quality of the CIGS/SDL interface has little impact on the performance of the cell. V_{oc} remains constant; J_{sc}, FF and efficiency decrease slightly for interface defect density ranging from 10^{12}
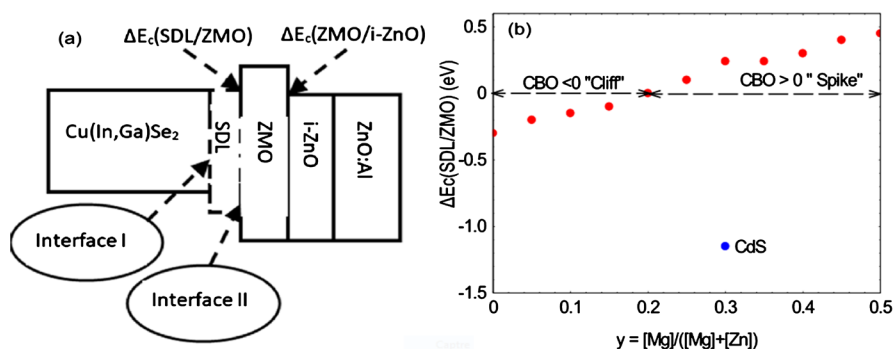

Figure 6. (a) Interface configurations for the simulation; (b) Variation of the conduction band offset at the SDL/ZMO interface as a function of Mg-content.

cm⁻² to 10¹³ cm⁻². Beyond a value of 10¹³ cm⁻² for the interface defect density, these electrical parameters become unaffected by the interface quality. However, the quality of the SDL/ZMO interface is crucial to the performance of the solar cell. This interface must be high quality to facilitate photo-generated electron transport in the absorber to the front contact. The simulation results show that the best performance is obtained when the defect density at this interface is less than 10¹⁴ cm⁻². Above this value, the parameters are stable at low values.

Figure 8 shows the evolution of the electrical parameters when the conduction band offset and the defect density at the SDL/ZMO interface are introduced as variables. For ΔE_c less than -0.1 eV, the open circuit voltage (V_{oc}) decreases with the depth of the cliff (**Figure 6(b)**) confirming that the cliff acts as a barrier for photo-generated electrons. Recombination between majority carriers via defects at the SDL/ZMO interface occurs due to this barrier, which leads to a decrease of V_{oc} with the depth of the cliff and the interface defect density at the SDL/ZMO interface [19]. Also, it has been shown that even small interface recombination velocities limit the open circuit voltage (V_{oc}) when the conduction band offset (ΔE_c) between window and absorber layer is close to zero or a negative value [22].

When a spike (**Figure 6(b)**) is formed at the SDL/ZMO interface, the barrier causing recombination decreases and the V_{oc} is not affected by SDL/ZMO interface quality. The short-circuit current density (J_{sc}) is strongly dependent on the defect density and conduction band alignment at the SDL/ZMO interface. The
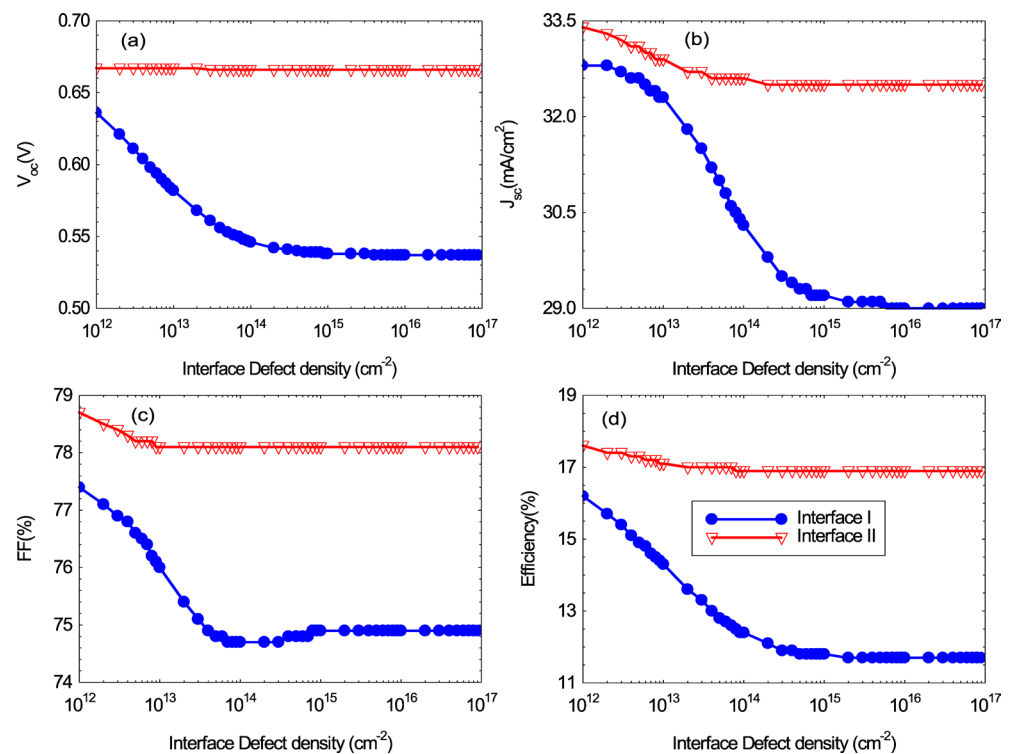

Figure 7. Effect of interface defect density on the electrical parameters: (a) V_{oc}; (b) J_{sc}; (c) FF and (d) Efficiency.
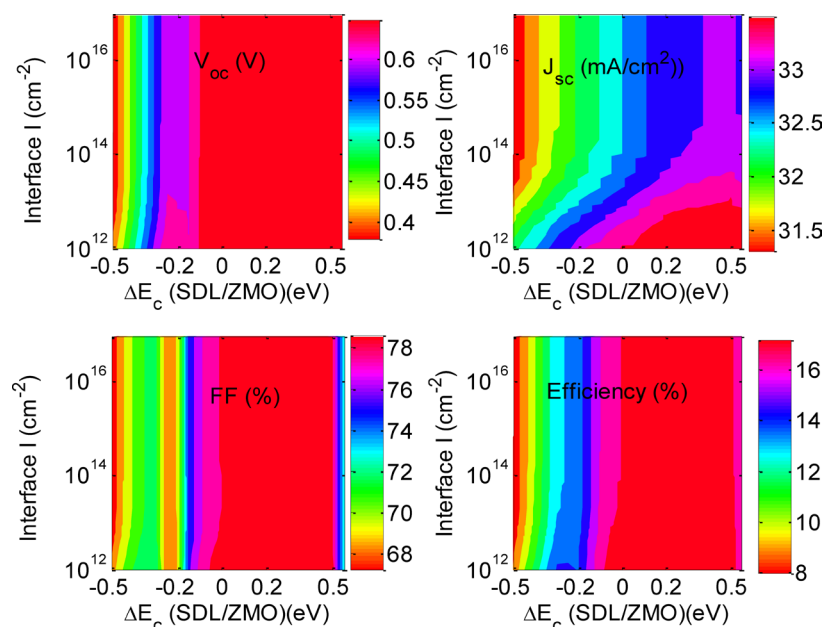
Figure 8. Effect of interface defect density and conduction band offset at the SDL/ZMO interface on V_{oc}, J_{sc}, FF and conversion efficiency.

best J_{sc} is obtained for positive conduction band offsets ($\Delta E_c > 0$) and interface defect densities below 10^{13} cm^{-2}. Interface defect densities greater than 10^{13} cm^{-2} combined with a strong cliff ($\Delta E_c < 0$) results in low J_{sc} cliffs below -0.1 eV result in low FF, regardless of the interface defect density. The same behavior occurs at high spike (>0.5 eV). Under these conditions, like V_{oc}, recombination at the SDL/ZMO interface limits the FF. A high conversion efficiency is obtained for a conduction band offset between 0 and 0.4 eV, regardless of the defect density at the SDL/ZMO interface.

4. Conclusion

Computer analysis is used to investigate the effect of ZMO mono-buffer layer on the performance of the CIGS solar cell. Courant-voltage (J-V) characteristic is used to explore the optimal properties of the ZMO layer such as thickness, donor density, magnesium concentration. Furthermore, the impact of Ga content on the performance of ZMO/CIGS hetero-junction has been investigated. The simulated results suggest that the Mg-content changes the band structure, while the Ga-content affects the absorber bulk defect properties. These changes could have a strong influence on the solar cell performance and could explain why the optimal contents of Mg and Ga for high CIGS solar cells, should be in the range of 0.15 - 0.2 and 0.4 respectively. In addition, ZMO/CIGS interface properties have been studied to elucidate how they affect device performance. The simulation results suggest that high interface defect density and unfavorable band alignment may be the causes of poor performances of Zn(Mg,O)/CIGS solar cells in the case of low and high Mg-contents. A comparison of the simulation results with published data for CIGS cells with Zn(Mg,O) buffer layer shows an

excellent agreement.

Acknowledgements

Conflicts of Interest

The authors declare no conflicts of interest regarding the publication of this paper.

References

[1] Nakamura, M., Yamaguchi, K., Kimoto, Y., Yasaki, Y., Kato, T. and Sugimoto, H. (2019) Cd-Free Cu(In,Ga)(Se,S)$_2$ Thin-Film Solar Cell with a New World Record Efficacy of 23.35%. *IEEE Journal of Photovoltaics*, **9**, 1863-1867. https://doi.org/10.1109/JPHOTOV.2019.2937218

[2] Stamford, L. and Azapagic, A. (2019) Environmental Impacts of Copper Indium Gallium Selenide (CIGS) Photovoltaics and the Elimination of Cadmium through Atomic Layer Deposition. *Science of the Total Environment*, **688**, 1092-1088. https://doi.org/10.1016/j.scitotenv.2019.06.343

[3] Siebentritt, S. (2011) What Limits the Efficiency of Chalcopyrite Solar Cells? *Solar Energy Materials and Solar Cells*, **95**, 1471-1476. https://doi.org/10.1016/j.solmat.2010.12.014

[4] Platzer-Björkman, C., Lu, J., Kessler, J. and Stolt, L. (2003) Interface Study of CuInSe$_2$/ZnO and Cu(In,Ga)Se$_2$/ZnO Devices Using ALD ZnO Buffer Layers. *Thin Solid Films*, **431-432**, 321-325. https://doi.org/10.1016/S0040-6090(03)00229-3

[5] Djinkwi Wanda, M., Ouédraogo, S. and Ndjaka, J.M.B. (2019) Theoretical Analysis of Minority Carrier Lifetime and Cd-Free Buffer Layers on the CZTS Based Solar Cell Performances. *Optik*, **183**, 284-293. https://doi.org/10.1016/j.ijleo.2019.02.058

[6] Hultqvist, A., Platzer-Björkman, C., Pettersson, J., Törndahl, T. and Edoff, M. (2009) CuGaSe$_2$ Solar Cells Using Atomic Layer Deposited Zn(O,S) and (Zn,Mg) O Buffer Layers. *Thin Solid Films*, **517**, 2305-2308. https://doi.org/10.1016/j.tsf.2008.10.109

[7] Hariskos, D., Fuchs, B., Menner, R., Naghavi, N., Hubert, C., Lincot, D. and Powalla, M. (2009) The Zn(S,O,OH)/ZnMgO Buffer in Thin-Film Cu(In,Ga)(Se,S)$_2$-Based Solar Cells Part II: Magnetron Sputtering of the ZnMgO Buffer Layer for In-Line Co-Evaporated Cu(In,Ga)Se$_2$ Solar Cells. *Progress in Photovoltaics: Research and Applications*, **17**, 479-488. https://doi.org/10.1002/pip.897

[8] Saadat, M., Moradi, M. and Zahedifar, M. (2015) Optimization of Zn(O,S)/(Zn,Mg)O Buffer Layer in Cu(In,Ga)Se$_2$ Based Photovoltaic Cells. *Journal of Materials Science: Materials in Electronics*, **27**, 1130-1133. https://doi.org/10.1007/s10854-015-3861-y

[9] Niemegeers, A. and Burgelman, M. (1996) Numerical Modelling of AC-Characteristics of CdTe and CIS Solar Cells. *Conference Record of the Twenty Fifth IEEE Photovoltaic Specialists Conference* 1996, Washington, DC, 13-17 May 1996, 901-904. https://doi.org/10.1109/PVSC.1996.564274

[10] Hernández-Como, N. and Morales-Acevedo, A. (2010) Simulation of Hetero-Junction Silicon Solar Cells with AMPS-1D. *Solar Energy Materials and Solar Cells*, **94**, 62-67. https://doi.org/10.1016/j.solmat.2009.05.021

[11] Dagamseh, A.M.K., Vet, B., Šutta, P. and Zeman, M. (2010) Modelling and Optimization of a-Si: H Solar Cells with ZnO: Al Back Reflector. *Solar Energy Materials and Solar Cells*, **94**, 2119-2123. https://doi.org/10.1016/j.solmat.2010.06.039

[12] Basore, P.A. and Clugston, D.A. (1996) PC1D Version 4 for Windows: From Analysis to Design. *Conference Record of the Twenty Fifth IEEE Photovoltaic Specialists Conference* 1996, Washington, DC, 13-17 May 1996. https://doi.org/10.1109/PVSC.1996.564023

[13] Singh, S., Kumar, S. and Dwivedi, N. (2012) Band Gap Optimization of p-i-n Layers of a-Si:H by Computer Aided Simulation for Development of Efficient Solar Cell. *Solar Energy*, **86**, 1470-1476. https://doi.org/10.1016/j.solener.2012.02.007

[14] Ouédraogo, S., Zougmoré, F. and Ndjaka, J.M.B. (2014) Computational Analysis of the Effect of the Surface Defect Layer (SDL) Properties on Cu(In,Ga)Se$_2$-Based Solar Cell Performances. *Journal of Physics and Chemistry of Solids*, **75**, 688-695. https://doi.org/10.1016/j.jpcs.2014.01.010

[15] Pettersson, J., Edoff, M. and Platzer-Björkman, C. (2012) Electrical Modeling of Cu(In,Ga)Se$_2$ Cells with ALD-Zn$_{1-x}$Mg$_x$O Buffer Layers. *Journal of Applied Physics*, **111**, 014509. https://doi.org/10.1063/1.3672813

[16] Pettersson, J., Platzer-Björkman, C., Hultqvist, A., Zimmermann, U. and Edoff, M. (2010) Measurements of Photo-Induced Changes in the Conduction Properties of ALD-Zn$_{1-x}$Mg$_x$O Thin Films. *Physica Scripta*, **2010**, 014010. https://doi.org/10.1088/0031-8949/2010/T141/014010

[17] Tobbeche, S., Kalache, S., Elbar, M., Kateb, M.N. and Serdouk, M.R. (2019) Improvement of the CIGS Solar Cell Performance: Structure Based on a ZnS Buffer Layer. *Optical and Quantum, Electronics*, **51**, Article No. 284. https://doi.org/10.1007/s11082-019-2000-z

[18] Sharbati, S., Keshmiri, S.H., McGoffin, J.T. and Geisthardt, R. (2014) Improvement of CIGS Thin-Film Solar Cell Performance by Optimization of Zn(O,S) Buffer Layer Parameters. *Applied Physics A*, **118** 1259-1265. https://doi.org/10.1007/s00339-014-8825-1

[19] Minemoto, T., Matsui, T., Takakura, H., Hamakawa, Y., Negami, T., Hashimoto, Y. and Kitagawa, M. (2001) Theoretical Analysis of the Effect of Conduction Band Offset of Window/CIS Layers on Performance of CIS Solar Cells Using Device Simulation. *Solar Energy Materials and Solar Cells*, **67**, 83-88. https://doi.org/10.1016/S0927-0248(00)00266-X

[20] Pettersson, J., Platzer-Björkman, C., Zimmermann, U. and Edoff, M. (2011) Baseline Model of Graded-Absorber Cu(In,Ga)Se$_2$ Solar Cells Applied to Cells with Zn$_{1-x}$Mg$_x$O Buffer Layers. *Thin Solid Films*, **519**, 7476-7480. https://doi.org/10.1016/j.tsf.2010.12.141

[21] Enayati Maklavani, S. and Mohammadnejad, S. (2020) Enhancing the Open-Circuit Voltage and Efficiency of CZTS Thin-Film Solar Cells Via band-offset Engineering. *Optical and Quantum Electronics*, **52**, Article No. 72. https://doi.org/10.1007/s11082-019-2180-6

[22] Gloeckler, M. and Sites, J.R. (2005) Efficiency limitations for Wide-Band-Gap Chalcopyrite Solar Cells. *Thin Solid Films*, **480-481**, 241-245. https://doi.org/10.1016/j.tsf.2004.11.018

[23] Minemoto, T., Hashimoto, Y., Satoh, T., Negami, T., Takakura, H. and Hamakawa, Y. (2001) Cu(In,Ga)Se$_2$ Solar Cells with Controlled Conduction Band Offset of Window/Cu(In,Ga)Se$_2$ Layers. *Journal of Applied Physics*, **89**, 8327-8330. https://doi.org/10.1063/1.1366655

[24] Minemoto, T., Hashimoto, Y., Shamskolahi, W., Satoh, T., Negami, T., Takakura, H. and Hamakawa, Y. (2003) Control of Conduction Band Offset in Wide-Gap Cu(In,Ga)Se$_2$ Solar Cells. *Solar Energy Materials and Solar Cells*, **75**, 121-126. https://doi.org/10.1016/S0927-0248(02)00120-4